Renewable Energy 36 (2011) 2032–2042

Contents lists available at ScienceDirect

Renewable Energy

journal homepage: www.elsevier.com/locate/renene

Technical Note

Adaptive pole-placement control of 4-leg voltage-source inverters for standalone photovoltaic systems

Reza Nasiri*, Ahmad Radan

Electrical Engineering Faculty, K.N. Toosi University of Technology, Seyed Khandan Bridge, 1431714191 Tehran, Iran

ARTICLE INFO

Article history:
Received 12 August 2010
Accepted 30 December 2010
Available online 20 January 2011

Keywords:
Photovoltaic systems
4-leg inverters
State feedback
Adaptive control
Self-tuner regulator
Pole-placement control strategy

ABSTRACT

Three-leg inverters for photovoltaic systems have many disadvantages, especially when the load is unbalanced. These disadvantages are, for example, small utilization of the DC link voltage, the dependency of the modulation factor of the load current and the superposition of a DC component with the output AC voltage. A solution for these problems is the 4-leg inverter. Most papers dealing with 4-leg inverters suggest classic controllers, such as PI controller, for the system. However, the transient performance of the closed-loop system does not become acceptable. On the other hand, adaptive control of 4-leg inverters has not yet been discussed in the literature. This paper proposes pole-placement control strategy, via state feedback, for 4-leg voltage-source inverters to adjust the transient performance of the closed-loop system. In addition, a STR (self-tuner regulator) is introduced to guarantee the adaptive performance of the controller in the presence of time-variant *RL* loads. Simulation results validate the theoretical results and proposed control strategy.

1. Introduction

The electrical energy gained from a photovoltaic (PV) system can be utilized in different ways. There are two kinds of the employment of solar modules, standalone [1,2] and grid coupled systems [11–13]. Standalone photovoltaic system [3–5] means that the system, composed of load and generator, is closed and locally limited [6,7]. The energy supply of a ship or a space chattel is gained from a standalone network. Grid coupled system [14–16] means that there is a supra-regional energy supply network [17] and the generated energy [18], for example, from a PV system [19] will be injected in this network [20]. Both operation modes must satisfy different requirements on the energy supply. In the standalone system [8], the problem to solve is to ensure the energy supply. As the solar energy supply works only, if there is sun radiation, the gained energy must be stored.

Photovoltaic generators can only produce DC currents and therefore only DC loads can be supplied [9]. To supply costumer AC loads an inverter unit must be applied. The inverter, which represents the interface between the photovoltaic generator and AC loads, is the main subject of this paper. Its task in context with standalone PV systems is to ensure the energy supply in three-phase standalone network.

The proposed standalone PV system is illustrated in Fig. 1. It consists of the PV generator, DC/DC1 converter, a battery energy storage, a second DC/DC2 converter, DC link capacitor bank, inverter, output filter and load. It can be seen that the proposed system is transformer less. For this reason a high DC link voltage is needed which is supplied with boost converter (DC/DC1). DC/DC2 is also a boost converter and acts as a maximum power point tracker (MPPT) [10] and battery charger. In this way the battery will be always charged at the maximum power point [10].

The goal of the system illustrated in Fig. 1 is to supply three as well as single-phase loads of any kind with constant amplitude sinusoidal voltage and constant frequency. To realize this, all three phases must be independent of each other. For this reason the neutral point of the LC output filter and load must be connected to a neutral point. There are many possibilities to realize this. One possibility, which is the 4-leg inverter, is shown in Fig. 2.

Because of additional neutral leg, 4-leg inverters are recommended for supplying unbalanced and/or nonlinear loads. Consequently, generation of balanced voltage, with sinusoidal waveform, is necessary for these inverters. As a result, using an appropriate load voltage controller is highly required.

To apply control techniques a DC operating point is needed. Thus, the transformation *T*, given in Appendix, is applied to the model of 4-leg inverter in *abc* coordinates to get the power stage model in rotating coordinates *dqo* [21–24].

* Corresponding author. Tel.: +98 21 84062408; fax: +98 21 88462066.
E-mail addresses: reza_nasiri80@yahoo.com (R. Nasiri), radan@kntu.ac.ir (A. Radan).

0960-1481/$ – see front matter © 2011 Elsevier Ltd. All rights reserved.
doi:10.1016/j.renene.2010.12.024

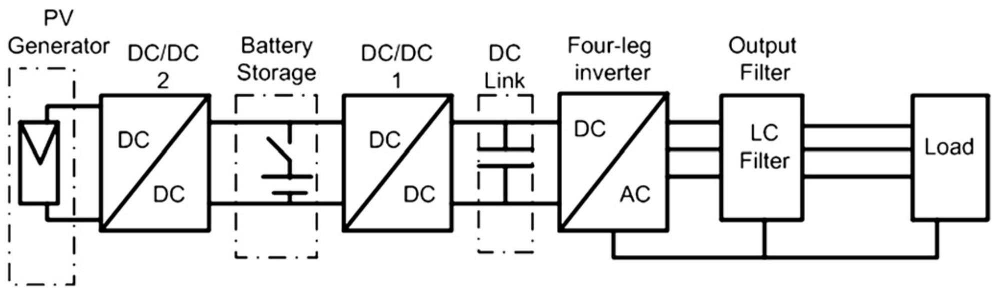

Fig. 1. Standalone photovoltaic system.

Most papers dealing with 4-leg inverters propose classic control techniques, such as PI controller, for the closed-loop system in rotating coordinates *dqo* [21–23]. But it has some drawbacks:

- Most classic control techniques use frequency domain factors, such as gain margin and phase margin, for designing. However, it cannot lead to a precise response in time domain. As a result, classic control techniques cannot adjust transient performance of the system such as overshoot and speed of response accurately. However, modern control techniques [24,25], like pole-placement control strategy, can be used for this aim.
- Designing in frequency domain is implicated. Moreover, classic control techniques design a controller only for one operating point while the load is time-variant, in practice. Consequently, the operating point varies with time. In other words, adaptive control techniques are required for 4-leg inverters. However, they have not yet been discussed for 4-leg inverters in the literature.

This paper solves all of the above problems as below.

1. It proposes pole-placement control strategy via state feedback [25], which is a modern control technique, to make the transient performance of the system greatly adjustable.
2. It introduces a STR (self-tuner regulator) [25], which is an adaptive control technique, to tune the controller when the load varies with time. Consequently, adaptive control of the final system is obtained.

This paper demonstrates that by using the proposed controller the 4-leg inverter generates balanced voltage in spite of the presence of *RL* time-variant loads. Additionally, the desired transient performance of the system is guaranteed. It should be noted that proposed control strategy can be used, similarly, for multilevel 4-leg inverters and other applications of the 4-leg structure, such as active power filters, but it is beyond the scope of this paper.

2. Four-leg inverters and their large-signal model

Fig. 2 shows the power stage model of the three-phase 4-leg voltage-source inverter with second-order load filter. The average model in *abc* stationary coordinates, without considering sampling delay, is shown in Fig. 3.

The output voltage and input current in the inverter can be represented as:

$$\begin{bmatrix} V_{af} & V_{bf} & V_{cf} \end{bmatrix}^T = \begin{bmatrix} d_{af} & d_{bf} & d_{cf} \end{bmatrix}^T \cdot V_{dc} \tag{1}$$

$$I_p = \begin{bmatrix} d_{af} & d_{bf} & d_{cf} \end{bmatrix} \cdot \begin{bmatrix} I_a & I_b & I_c \end{bmatrix}^T \tag{2}$$

where V_{if} ($i = a, b, c$) the inverter output voltages (line-neutral), I_i ($i = a, b, c$) are line currents. And, d_{in} ($i = a, b, c$) are line-to-neutral duty ratios.

The duty ratios d_{in} ($i = a, b, c$) are controlled in a way so as to produce sinusoidal voltages at output of the filter, irrespective of the load. The system requirement can be expressed as:

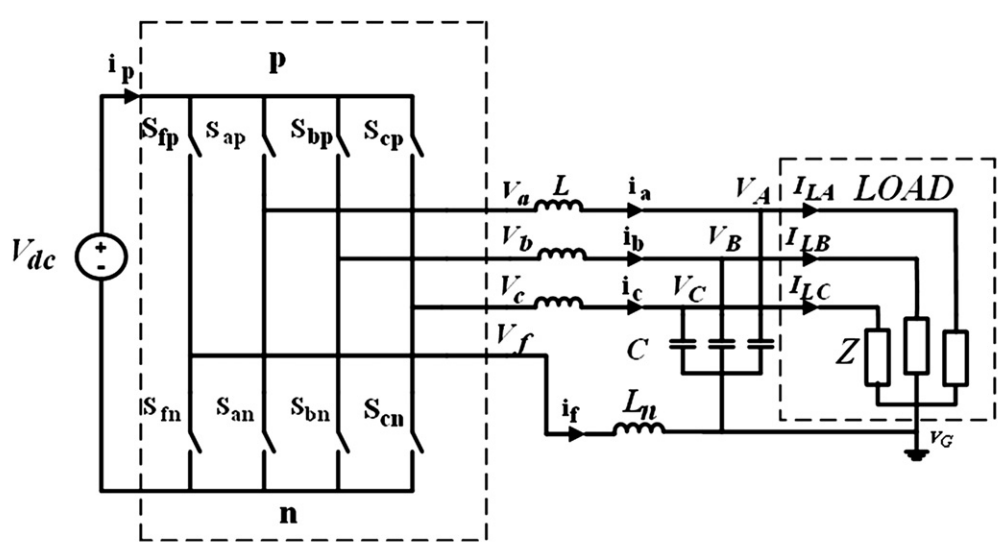

Fig. 2. Four-leg voltage-source inverter.

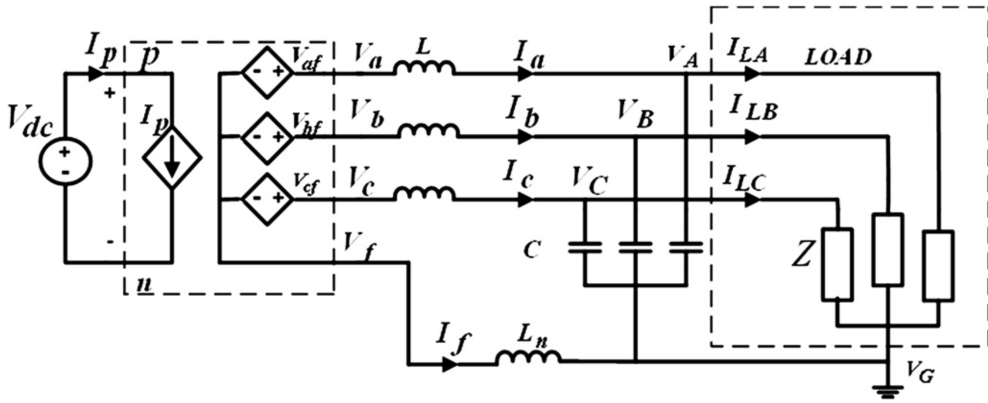

Fig. 3. Average large-signal model of the 4-leg inverter with LC filter.

$$\begin{bmatrix} V_{AG} \\ V_{BG} \\ V_{CG} \end{bmatrix} = V_{\mathrm{m}} \begin{bmatrix} \cos(\omega t) \\ \cos(\omega t - 120^\circ) \\ \cos(\omega t + 120^\circ) \end{bmatrix} \tag{3}$$

where V_{iG} $(i = A, B, C)$ is the output load voltage and, V_{m} is the rated output voltage.

3. Control structure for load voltage control

3.1. Power stage model of the 4-leg inverter with RL load neglecting coupling

To produce the desired sinusoidal output voltages, the steady-state duty ratios are time-varying and sinusoidal. But to apply control techniques a DC operating point is needed.

Thus, the transformation *T*, given in Appendix, is applied to get the power stage model in rotating coordinates. In addition, the load is assumed to be *RL* and time-invariant. Fig. 4 gives the power stage model in rotating coordinates. The *d* and *q* sub-circuits have coupled voltage and current sources.

The steady-state output load voltages are DC quantities and are given as:

$$\begin{bmatrix} V_d \\ V_q \\ V_o \end{bmatrix} = \begin{bmatrix} V_{\mathrm{m}} \\ 0 \\ 0 \end{bmatrix} \tag{4}$$

where V_{m} is the rated output voltage.

For balanced *RL* load we have

$$R_d = R_q = R_o = R_a = R_b = R_c = R$$
$$L_d = L_q = L_o = L_a = L_b = L_c = L'$$

where R is resistance and L' is the inductance of the load. R_a, R_b, and R_c are the resistance of the load in phases (a, b, c) and R_d, R_q, R_o are equivalent resistance of the load in rotating coordinate *dqo*.

The power stage is a coupled multi-variable multi-loop system. The coupling between the *d* and *q* channels of the power stage is shown in Fig. 4. Coupling is neglected and independent control of the system is presented. Fig. 5 shows the control structure for load voltage loop control.

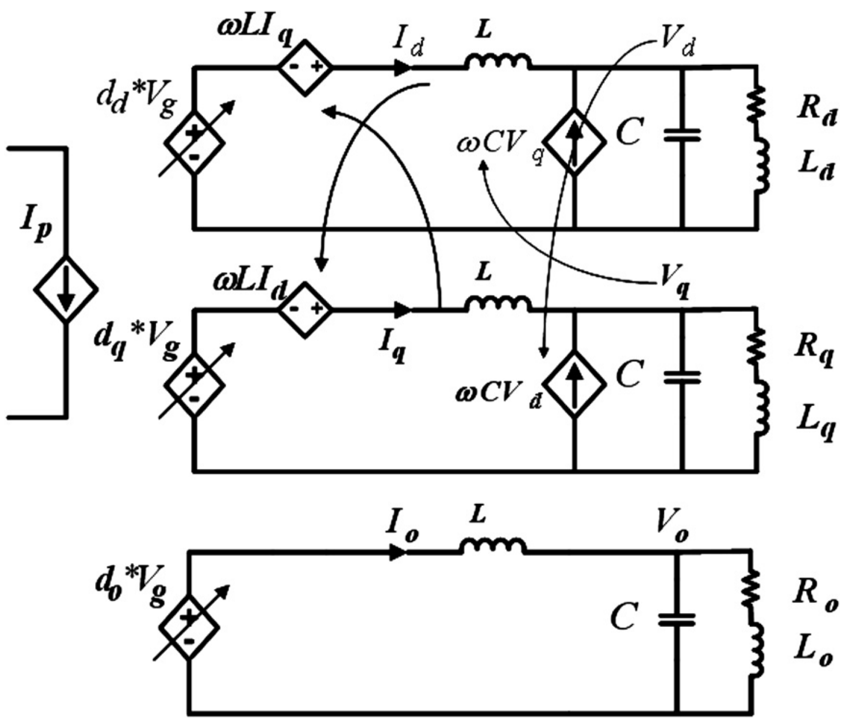

Fig. 4. Power stage average model in rotating coordinates: The *d* and *q* sub-circuits have coupled voltage and current sources.

3.2. Realization of the proposed power stage model

The signal flow graph of the inverter, shown in Fig. 5, is realized as Fig. 6. Consequently, the state-space equations of the system for d channel are expressed as:

$$\begin{aligned} \dot{x} &= A \cdot x + B \cdot u \\ Y &= C \cdot x \end{aligned} \tag{5}$$

where,

$$x = \begin{bmatrix} i_{Ld} \\ V_d \\ i_d \end{bmatrix}, C = \begin{bmatrix} 0 & 1 & 0 \end{bmatrix}, B = \begin{bmatrix} \frac{V_g}{L} \\ 0 \\ 0 \end{bmatrix}$$

and

$$A = \begin{bmatrix} 0 & -\frac{1}{L} & 0 \\ 0 & \frac{1}{L_d} & -\frac{R_d}{L_d} \\ \frac{1}{C} & 0 & -\frac{1}{C} \end{bmatrix}$$

Equations are expressed for the d channel in this and next sections. It is evident that the q and o channels equations are similar to the d one.

4. Pole-placement control strategy via state feedback and static lead compensator

Let the controller has the linear state feedback form

$$u = -K \cdot x + G \cdot r \tag{6}$$

where $r \in R$ is a new vector with 1 input and K, state feedback, and G, static lead compensator, are the unknown controller matrices with dimensions 1×3 and 1×1, respectively (Fig. 7).

Substituting Eq. (6) in Eq. (5) yields the closed-loop system

$$\begin{aligned} \dot{x} &= (A - BK)x + BGr \\ y &= Cx \end{aligned} \tag{7}$$

The control problem is to determine the control law (6), to determine the controller matrices K and G, such that the closed-loop system has the desired characteristics.

4.1. Pole-placement via state feedback

Consider the linear, time-invariant system

$$\dot{x}(t) = Ax(t) + Bu(t) \tag{8}$$

where all states are accessible and known. To this system, a linear state feedback control law of the below form is applied

$$u(t) = -Kx(t) \tag{9}$$

Then, the closed-loop system, Fig. 7, is given by the homogeneous Eq. (10)

$$\dot{x}(t) = (A - BF)x(t) \tag{10}$$

Here, the design problem is to find the appropriate controller matrix so as to improve the performance of the closed-loop system Eq. (10). One such method of improving the performance of (10) is that of pole-placement. The pole-placement method consists of finding a particular matrix K, such that the poles of the closed-loop (10) take on desirable pre-assigned values. Using this method, the

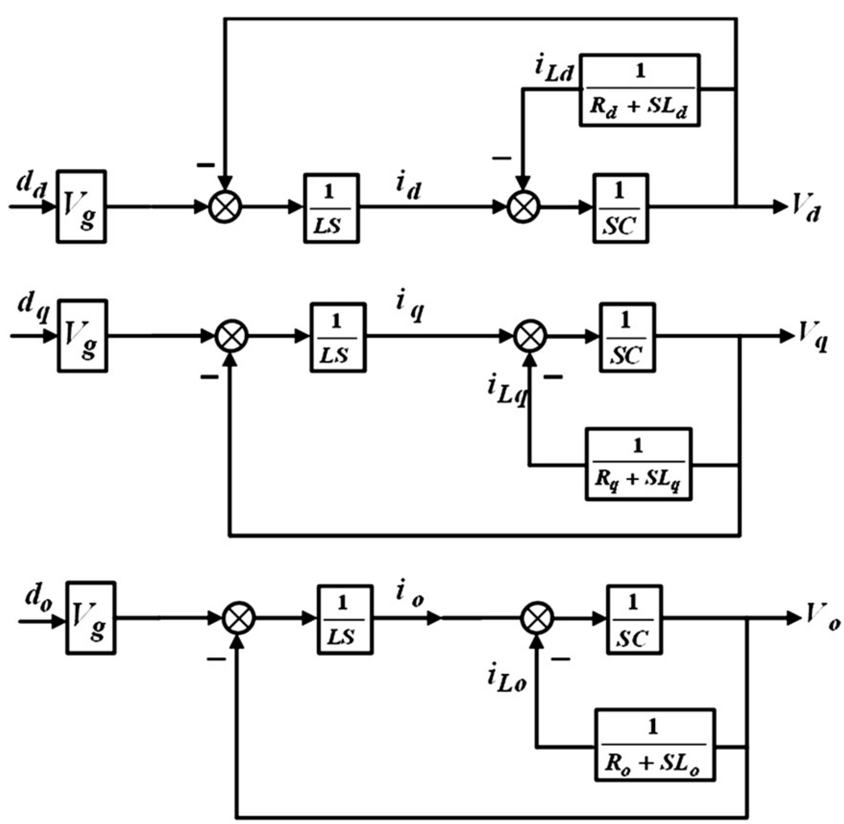

Fig. 5. Average model represented as signal flow graph; coupling has been neglected.

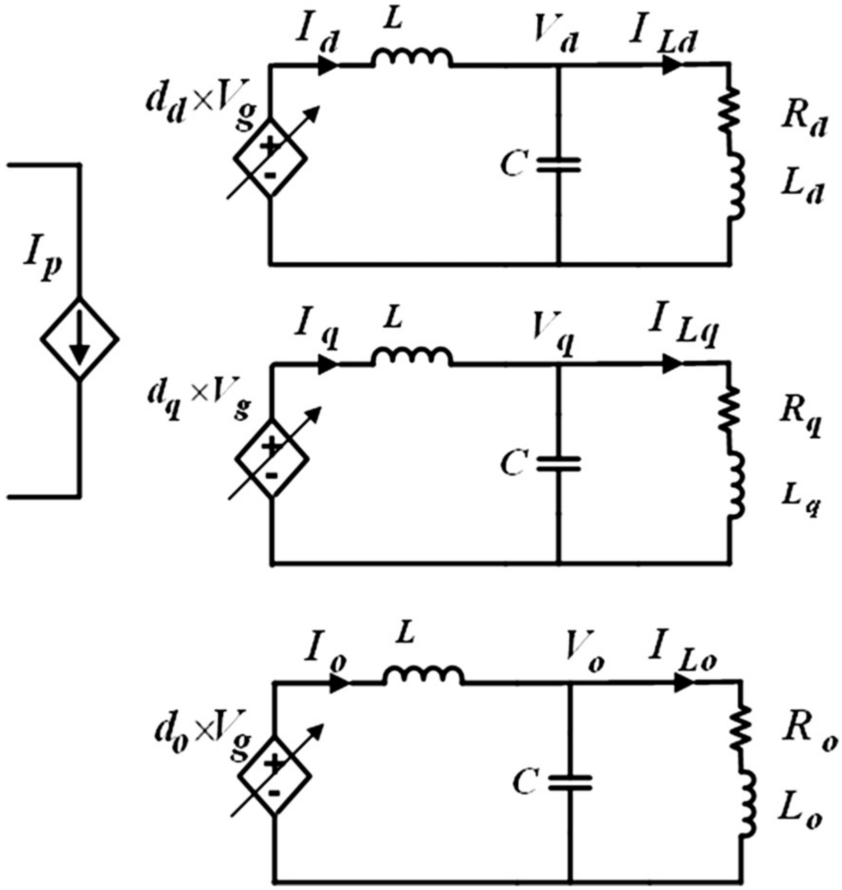

Fig. 6. Average model represented as signal flow graph; coupling has been neglected.

behavior of the open-loop system may be improved significantly. For example, the method can stabilize an unstable system, increase or decrease the speed of response and so on. For this reason, improving the system performance via the pole-placement method is widely recommended.

The pole-placement or eigenvalue assignment problem can be defined as follows: let λ_1, λ_2, λ_3 be the eigenvalues of the matrix A of the open-loop system (8) and $\widehat{\lambda}_1, \widehat{\lambda}_2, \widehat{\lambda}_3$ be the desired eigenvalues of the matrix $A - BK$ of the closed-loop system (10), where all complex eigenvalues exist in complex conjugate pairs. Also, let $p(s)$ and $\widehat{p}(s)$ be the respective characteristic polynomials, i.e., let us find a matrix K so that

$$p(s) = \prod_{i=1}^{4}(s-\lambda_i) = |sI - A| = s^3 + a_2 s^2 + a_1 s + a_0 \tag{11}$$

$$\widehat{p}(s) = \prod_{i=1}^{4}\left(s-\widehat{\lambda}_i\right) = |sI - A + BK| = s^3 + \alpha_2 s^2 + \alpha_1 s + \alpha_0 \tag{12}$$

Eq. (12) is satisfied. The controllability matrix Φ_c of system (8) can be expressed as:

$$\Phi_c = \begin{bmatrix} B & \vdots & AB & \vdots & A^2B \end{bmatrix} = \begin{bmatrix} \frac{V_g}{L} & 0 & 0 \\ 0 & 0 & -\frac{R_d V_g}{L_d LC} \\ 0 & \frac{V_g}{LC} & -\frac{V_g}{LC^2} \end{bmatrix} \tag{13}$$

It is evident that $\text{rank}(\Phi_c) = 3$, for $R_d \neq 0$. Therefore, the system (A, B) is controllable, a fact which guarantees that there exists a matrix K which satisfies the pole-placement problem.

Several methods have been proposed for determining K. One of the most popular pole-placement methods is *the Base–Gura Formula* which gives the following simple solution:

$$K = (\alpha - a)\psi^{-1}\Phi_c^{-1} \tag{14}$$

where Φ_c is the controllability matrix, defined in Eq. (13), and

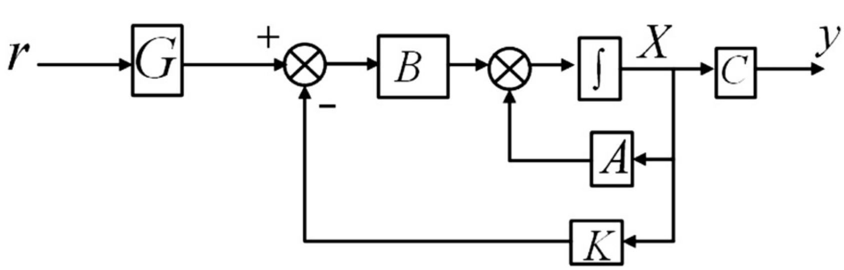

Fig. 7. Block diagram of the pole-placement control strategy via state feedback, K, with static lead compensator, G.

$$\psi = \begin{bmatrix} 1 & a_2 & a_1 \\ 0 & 1 & a_2 \\ 0 & 0 & 1 \end{bmatrix}, \alpha = [\alpha_2 \quad \alpha_1 \quad \alpha_0], a = [a_1 \quad a_2 \quad a_0],$$

$$K = [K_{11} \quad K_{12} \quad K_{13}]$$

By substituting A, B and Φ_c, state feedback matrix K can be expressed as:

$$K = (\alpha - a)\begin{bmatrix} \frac{L}{V_g} & -\frac{LCa_2}{LCV_g} & \frac{LCL_d(a_1 - a_2^2)}{R_d V_g} + \frac{LL_d a_2}{R_d V_g} \\ 0 & \frac{LC}{V_g} & \frac{LCL_d a_2 - LL_d}{R_d V_g} \\ 0 & 0 & -\frac{LCL_d}{R_d V_g} \end{bmatrix} \tag{15}$$

4.2. Input reference tracking via static lead compensator

The poles of the system are assigned in every place by using state feedback method, which was presented in previous section. However, the system does not track the reference input. To do this, a static lead compensator which is the matrix G is used. To guarantee the tracking performance of the system (7) we have

$$\lim_{t \to \infty} y(t) = r \tag{16}$$

On the other hand when $t \to \infty$, Eq. (7) is given by

$$\begin{aligned} \dot{x}(\infty) &= 0 = (A - BK)x(\infty) + BGr \\ y(\infty) &= Cx(\infty) \end{aligned} \tag{17}$$

By substituting Eq. (16) in Eq. (17), G can be expressed as:

$$G = -C(A - BK)^{-1}B \tag{18}$$

The matrix G is obtained by substituting A, B, C and K, as follow.

$$G = \left(\frac{L \cdot C \cdot T \cdot \alpha_0 \cdot L_d}{V_g \cdot R_d}\right) \tag{19}$$

Fig. 7 shows the diagram of the final control strategy. This system has poles, which are assigned by the matrix K, and tracks the input by G.

5. Adaptive control via a self-tuner regulator

In the previous sections, the system was assumed to be time-invariant. Proposed strategy works only for one operating point. However, in practical systems the load is usually time-variant, i.e. R_d and L_d vary with time.

To solve this problem, the matrix K and scalar G are defined as functions of R_d and L_d as follows

$$K_{1j} = f_{1j}(R_d, L_d) \tag{20}$$

$$G = f(R_d, L_d) \tag{21}$$

where ($j = 1, 2, 3$).

Then, a self-tuner regulator is used to tune the matrices K and G. Using this method, adaptive control of the system is guaranteed.

Fig. 8 depicts the proposed self-tuning strategy. The voltage and current of the load are sampled and the resistant and inductance of the load, R_d and L_d, are calculated and goes thorough the STR. Then STR calculates matrices K and G and tunes the system. Consequently, the final system works adaptively.

Now, the problem is to define the matrix K and scalar G as functions of R_d and L_d.

Consider the Eq. (11) as follows:

$$|sI - A| = s^3 + a_2 \cdot s^2 + a_1 \cdot s + a_0 \tag{22}$$

By substituting A in Eq. (22) we have:

$$\begin{aligned} a_2 &= \frac{R_d}{L_d} \\ a_1 &= \frac{1}{LC} + \frac{1}{L_d C} \\ a_0 &= \frac{R_d}{LCL_d} \end{aligned} \tag{23}$$

By substituting Eq. (23) in Eq. (15) the matrix K can be expressed as:

$$K_{11} = f_{11} = \left(-\frac{L}{V_g}\right)\frac{R_d}{L_d} + \frac{L \cdot \alpha_2}{V_g}$$

$$K_{12} = f_{12} = \left(\frac{L \cdot C}{V_g}\right)\frac{R_d^2}{L_d^2} + \left(-\frac{L \cdot C \cdot \alpha_2}{V_g}\right)\frac{R_d}{L_d} + \left(-\frac{L}{V_g}\right)\frac{1}{L_d} + \left(\frac{L \cdot C \cdot \alpha_1}{V_g} - \frac{1}{V_g}\right)$$

$$\begin{aligned} K_{13} = f_{13} = {} & \left(-\frac{L \cdot C}{V_g}\right)\frac{R_d^3}{L_d^2} + \left(\frac{L \cdot C \cdot \alpha_2}{V_g}\right)\frac{R_d^2}{L_d} + \left(\frac{2 \cdot L}{V_g}\right)\frac{R_d}{L_d} \\ & + \left(-\frac{L \cdot C \cdot \alpha_1}{V_g}\right)R_d + \left(\frac{L \cdot C \cdot \alpha_0}{V_g}\right)L_d + \left(-\frac{L \cdot \alpha_2}{V_g}\right) \end{aligned} \tag{24}$$

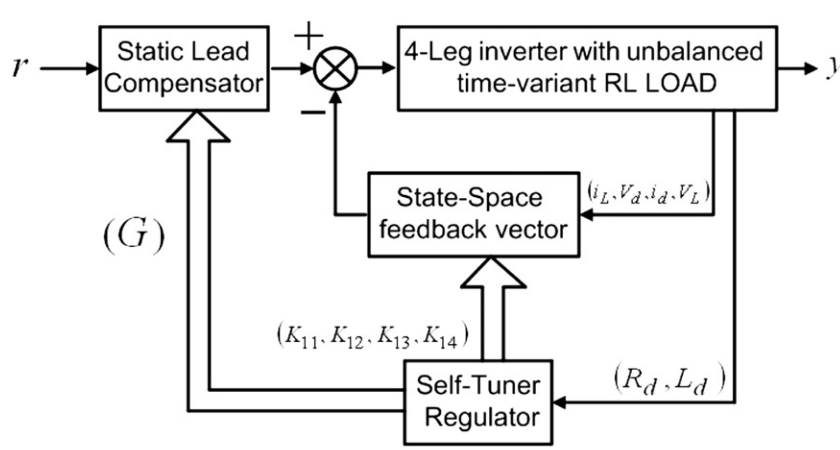

Fig. 8. Self-tuner regulator strategy.

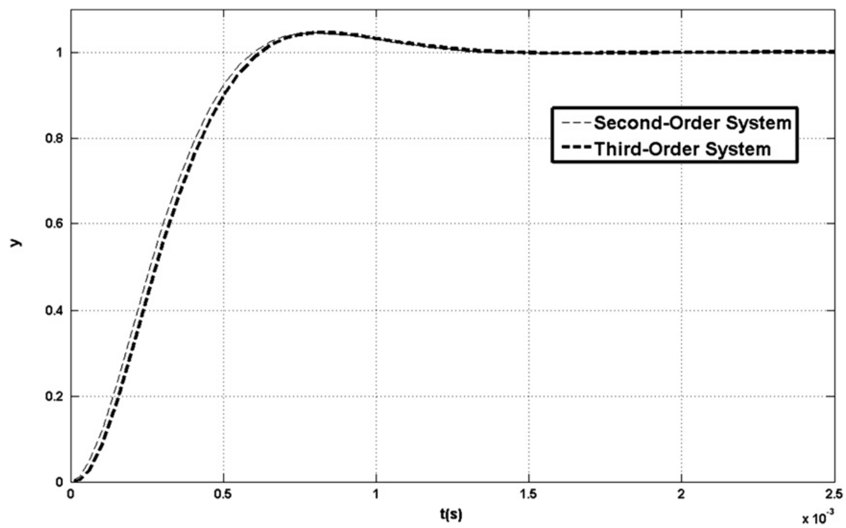

Fig. 9. Time response of the desired second-order and third-order systems when the input is unit step.

And for scalar G we have

$$G = f(R_d, L_d) = \left(\frac{L \cdot C \cdot \alpha_0}{V_g}\right)\frac{L_d}{R_d} \tag{25}$$

The resulting formulas are used by STR after sampling the voltage and current of the load and calculation of R_d and L_d.

The proposed strategy is simple to implement in digital devices because it needs sampling, like other control strategies, and simple calculation containing product, sum, subtract and division. Moreover, it tracks steady-state response with desired transient performance behavior in presence of unbalanced resistive–inductive (R–L) time-variant loads.

6. Simulation results and discussion

In this section, the performance of the proposed control strategy is investigated by a computer simulation using SIMULINK-MATLAB software.

The system parameters specifications used in the simulation are as follows:

$L = 333\ \mu\text{H}$

$C = 100\ \mu\text{H}$

$R_d = R_q = R_o = 100\ \Omega$

$L_d = L_q = L_o = 200\ \mu\text{H}$

$V_g = 800$ v

$V_m = 400$ v

The best PI controller's parameters:

$$K_i = 0.07, K_p = 1.2 \times 10^{-7}$$

6.1. Desired characteristic equation

The desired respective characteristic polynomial for proposed model has 3 poles, or 3 eigenvalues. Two poles are assumed to be complex. Therefore, they are considered, together, as a second-

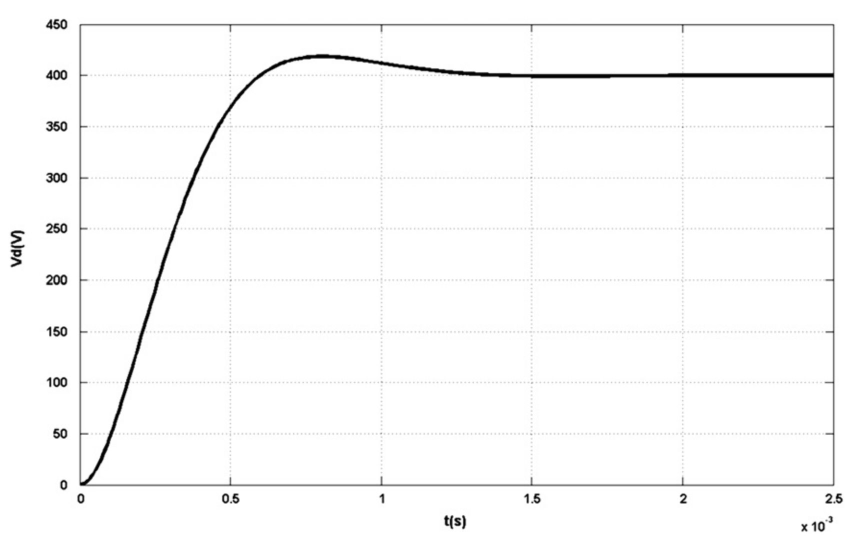

Fig. 10. Time response of the closed-loop system with proposed control strategy.

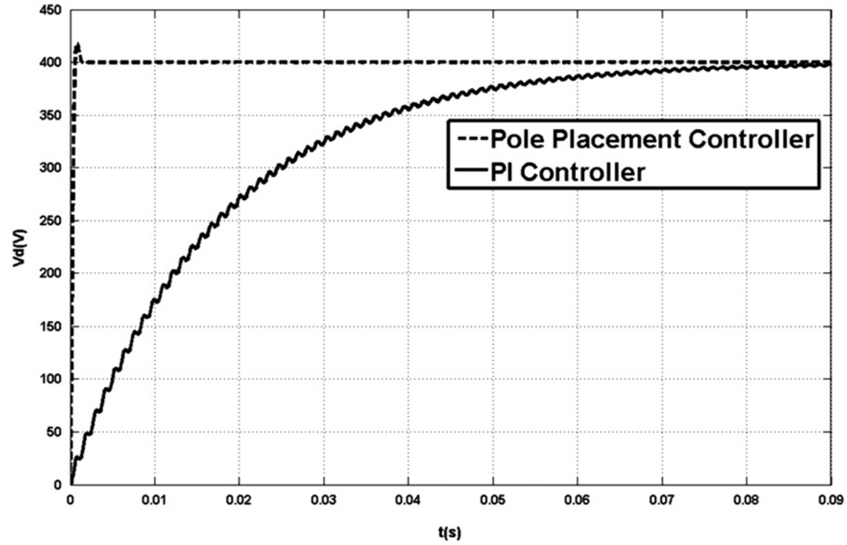

Fig. 11. Time response of the closed-loop system for PI controller and proposed controller.

order system. Another pole is assumed to be real and located far from the second-order system's poles. Therefore, its effect is ignored on the final, third-order system.

To have an acceptable overshoot and a very high speed of response, a second-order system with $\zeta = 0.69$ and $\omega_n = 5480$, (26), is ideal. In addition, another pole, which is located in $s = -50{,}000$, guarantees that the behavior of the resulting, third-order, system (27), is matched with the behavior of the second-order system (26)

$$G_2 = \frac{\omega_n^2}{s^2 + 2\cdot\zeta\cdot\omega_n + \omega_n^2} = \frac{5480^2}{s^2 + 2\times 0.69\times 5480 s + 5480^2} \tag{26}$$

$$\begin{aligned} G_3 &= \frac{p\omega_n^2}{(s+p)\left(s^2 + 2\zeta\omega_n + \omega_n^2\right)} \\ &= \frac{50000 \times 5480^2}{(s+50000)\left(s^2 + 2 \times 0.69 \times 5480 + 5480^2\right)} \end{aligned} \tag{27}$$

$$G_3 = \frac{50000 \times 5480^2}{s^3 + \alpha_2 \cdot s^2 + \alpha_1 \cdot s + \alpha_0} \tag{28}$$

Thus, the respective characteristic polynomial of the desired system can be expressed as:

$$\widehat{p}(s) = s^3 + \alpha_2 \cdot s^2 + \alpha_1 \cdot s + \alpha_0 \tag{29}$$

where

$$\begin{aligned} \alpha_2 &= 257702756150 \\ \alpha_1 &= 1.9482160658648 \times 10^{15} \\ \alpha_0 &= 7.5090094293545 \times 10^{18} \end{aligned}$$

Fig. 9 shows the time response of the proposed second-order system (26) and the desired third-order system (27) for the unit step input. It can be seen that the time response of the third-order system is matched with the second one. It should be noted that the systems, (26) and (27), have an overshoot equal to 5% and the time of response less than 0.0015 ms. This system (27) is chosen as our desired system.

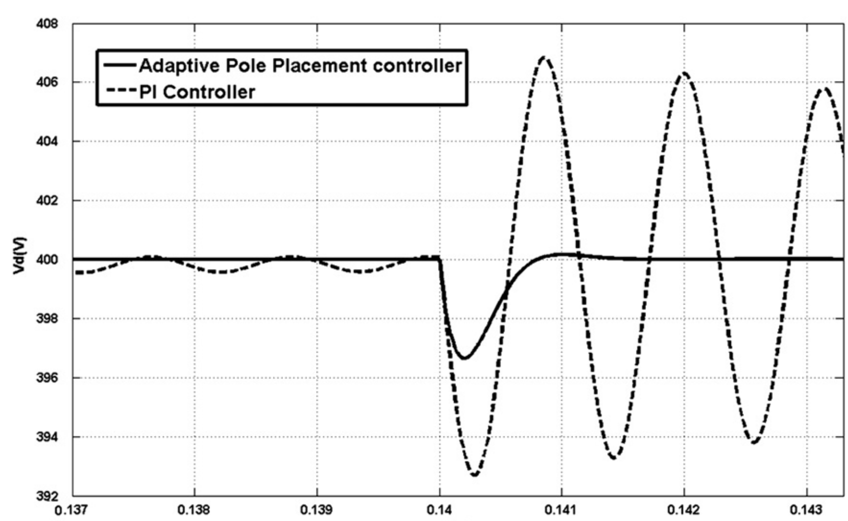

Fig. 12. The time response of the closed-loop system with PI controller and proposed controller when at the time $t = 0.14$ s, suddenly, R_d: 100 Ω → 50 Ω and L_d: 0.0002H → 0.0001H.

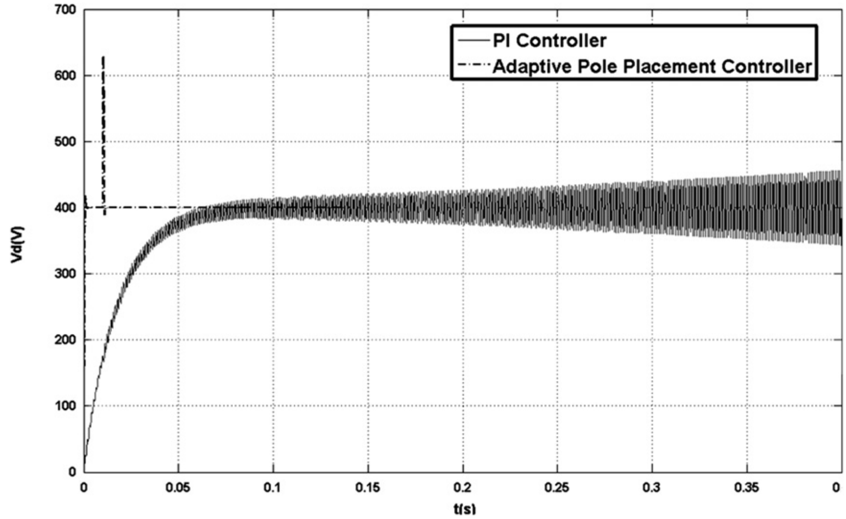

Fig. 13. The time response of the closed-loop systems with PI controller and proposed controller when at the time $t = 0.01$ s, suddenly, R_d: 100 Ω → 10 Ω and L_d: 0.0002H → 0.008H.

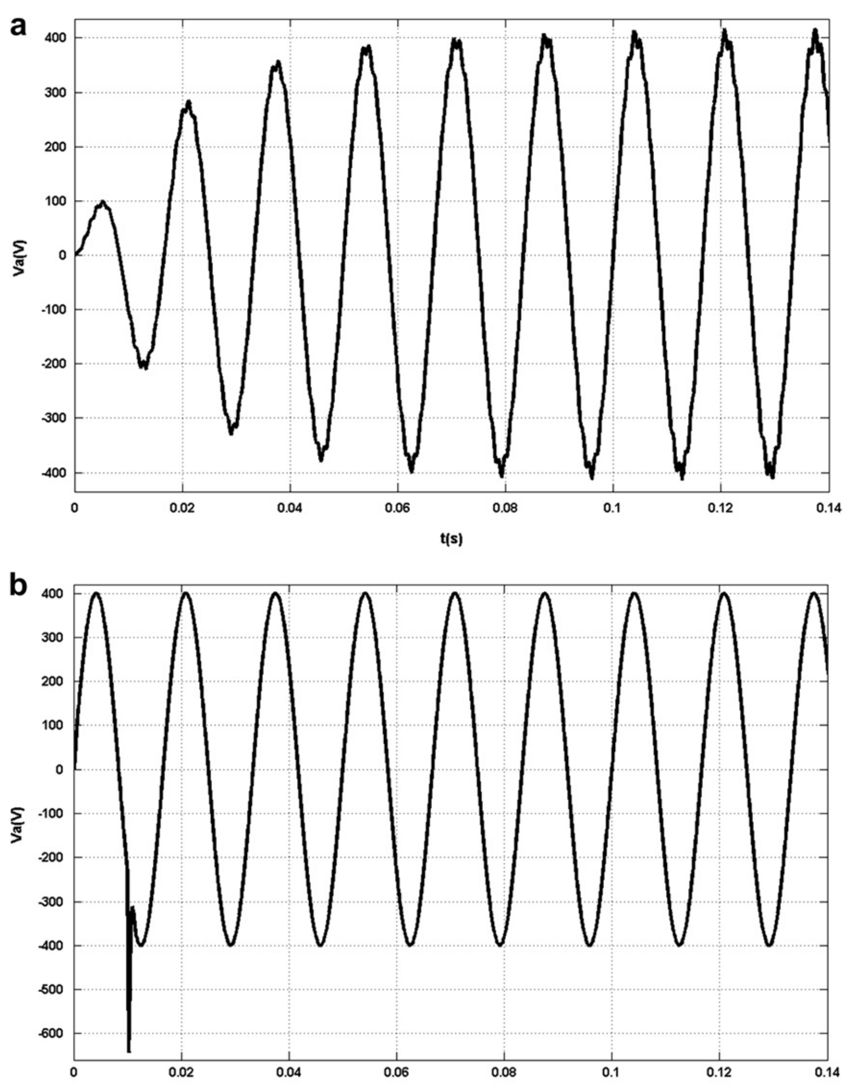

Fig. 14. Voltage phase a across when at the time t = 0.01 s, suddenly, R_d: 100 Ω → 10 Ω and L_d: 0.0002H → 0.008H: (a) PI controller; and (b) proposed controller.

6.2. Time response of the closed-loop system with proposed control strategy to step unit input

Fig. 10 depicts the time response of the closed-loop system with proposed control strategy. As expected, the output voltage tracks the reference input ($V_{\text{d-reference}} = V_{\text{m}} = 400\,\text{V}$) in steady-state conditions. Additionally, the transient performance of the system, such as overshoot and speed of response, is matched with the desired third-order system (27), shown in Fig. 9, which was presented in previous subsection. Consequently, this simulation validates the theoretical results.

6.3. Comparison between proposed controller and PI controller

Fig. 11 depicts the response of the system with proposed pole-placement control strategy and with PI controller ($K_p = 0.07$, $K_i = 0.001$) in a picture, for comparison. The PI controller has a very slow response. It tracks the input after 3 cycles (0.09 s). However, the system with state feedback vector tracks the input less than 0.0015 s.

6.4. Adaptive performance

To test the adaptive performance of the proposed control strategy, we assume that at the time $t = 0.14$ s, suddenly, R_d: 100 Ω → 50 Ω and L_d: 0.0002H → 0.001H. Fig. 12 depicts the transient performance of the PI controller and adaptive pole-placement control strategies. It shows that the adaptive type has the better response in transient conditions because it has less overshoot and more speed of response.

As another case we assume that at $t = 0.01$ s, suddenly, R_d: 100 Ω → 10 Ω and L_d: 0.0002H → 0.008H. Fig. 13 shows the response of the PI control strategy and adaptive control strategy. The PI controller cannot stabilize the system and it becomes unstable. However, proposed adaptive controller stabilizes the system and tracks the reference input with a high speed. Altogether, the performance of the system is acceptable. It should be noted that we have applied an extreme change in load. Fig. 14 shows the equivalent voltage of phase *a* across the load.

7. Conclusion

The task of a 4-leg voltage-source inverter for standalone photovoltaic systems is to produce symmetrical three-phase sinusoidal voltages from a DC voltage-source, so that a constant three and single-phase loads can be supplied with AC voltage with constant amplitude frequency. Unfortunately, the consumers in a standalone power supply network are unknown and underlie an arbitrary load profile. In many cases the load is *RL* and time-variant. From the control point of view the load current affects both the output voltage and the inductance current of the output filter. There are many possibilities to control such a system. Most papers dealing with 4-leg inverters suggest classic controllers, such as PI controller, for the system. However, the transient performance of the closed-loop system does not become acceptable. In addition, adaptive control of 4-leg inverters has not yet been discussed in the literature.

Modern control theory, which uses state equations for controller design, offers precise control in time domain. However, it has not yet been noticed for 4-leg inverter's controller design. This paper proposes it as a suitable approach in the 4-leg inverter case. Moreover, it demonstrates unique advantages of this approach.

This paper presents an adaptive pole-placement control strategy for 4-leg voltage-source inverters. It applies state feedback to the 4-leg inverter system, assuming the load is balanced *RL* time-invariant. Then, it obtains equations that get the feedback vector. In addition, feedback vector is defined as a function of the load. Consequently, a STR is used to tune the feedback vector, when the load is time-variant. All of the equations are simple and implementation of the proposed control strategy in practice is simple, too. In conclusion, the following can be made.

- The proposed technique guarantees tracking of the reference input in steady-state conditions.
- The performance of closed-loop system in the transient state conditions is adjustable by using this control strategy.
- The proposed control strategy is static and very simple. As a result, the design and implementation of the controller becomes highly simple.

Appendix

Stationary to rotating coordinates transformation:

$$\begin{bmatrix} V_d \\ V_q \\ V_o \end{bmatrix} = \begin{bmatrix} V_\alpha \\ V_\beta \\ V_\gamma \end{bmatrix} = \frac{2}{3}\begin{bmatrix} 1 & -\frac{1}{2} & -\frac{1}{2} \\ 0 & \frac{\sqrt{3}}{2} & -\frac{\sqrt{3}}{2} \\ \frac{1}{2} & \frac{1}{2} & \frac{1}{2} \end{bmatrix}\begin{bmatrix} V_a \\ V_b \\ V_c \end{bmatrix}$$

References

[1] Ilango GS, Rao PS, Karthikeyan A, Nagamani C. Single-stage sine-wave inverter for an autonomous operation of solar photovoltaic energy conversion system. Renew Energy 2010;35:275–82.
[2] Kim H-S, Kim J-H, Min B-D, Yoo D-W, Kim H-J. A highly efficient PV system using a series connection of DC–DC converter output with a photovoltaic panel. Renew Energy 2009;34:2432–6.
[3] Yu B, Matsui M, Jung Y, Yu G. A combined active anti-islanding method for photovoltaic systems. Renew Energy 2008;33:979–85.
[4] Mellit A, Benghanem M, Kalogirou SA. Modeling and simulation of a stand-alone photovoltaic system using an adaptive artificial neural network: proposition for a new sizing procedure. Renew Energy 2007;32:285–313.
[5] Kaviani AK, Riahy GH, Kouhsari SHM. Optimal design of a reliable hydrogen-based stand-alone wind/PV generating system considering component outages. Renew Energy 2009;34:2380–90.
[6] Kolhe M, Agbossou K, Hamelin J, Bose TK. Analytical model for predicting the performance of photovoltaic array coupled with a wind turbine in a stand-alone renewable energy system based on hydrogen. Renew Energy 2003;28:727–42.
[7] Hrayshat ES. Brackish water desalination by a stand alone reverse osmosis desalination unit powered by photovoltaic solar energy. Renew Energy 2008;33:1784–90.
[8] Celik AN. Effect of different load profiles on the loss-of-load probability of stand-alone photovoltaic systems. Renew Energy 2007;32:2096–115.
[9] Mellit A, Kalogirou SA, Shaari S, Salhi H, Arab AH. Methodology for predicting sequences of mean monthly clearness index and daily solar radiation data in remote areas: application for sizing a stand-alone PV system. Renew Energy 2008;33:1570–90.
[10] Li C-H, Zhu X-J, Cao G-Y, Sui S, Hu M-R. Dynamic modeling and sizing optimization of stand-alone photovoltaic power systems using hybrid energy storage technology. Renew Energy 2009;34:815–26.
[11] Notton G, Lazarov V, Stoyanov L. Optimal sizing of a grid-connected PV system for various PV module technologies and inclinations inverter efficiency characteristics and locations. Renew energy 2010;35:541–54.
[12] Nofuentes G, Almonacid G. An approach to the selection of the inverter for architecturally integrated photovoltaic grid-connected systems. Renew Energy 1998;15:487–90.
[13] Rahim NA, Selvaraj J, Krismadinata C. Five-level inverter with dual reference modulation technique for grid-connected PV system. Renew Energy 2010;35:712–20.
[14] Hassaine L, Olias E, Quintero J, Haddadi M. Digital power factor control and reactive power regulation for grid-connected photovoltaic inverter. Renew Energy 2009;34:315–21.
[15] Salas V, Alonso-Abella M, Chenlo F, Olias E. Analysis of the maximum power point tracking in the photovoltaic grid inverters of 5 KW. Renew Energy 2009;34:2366–72.
[16] Calais M, Agelidis VG, Dymond MS. A cascaded inverter for transformer less single-phase grid-connected photovoltaic systems. Renew Energy 2001;22:255–62.
[17] Gounden NA, Peter SA, Nallandula H, Krithiga S. Fuzzy logic controller with MPPT using line-commutated inverter for three-phase grid-connected photovoltaic systems. Renew Energy 2009;34:909–15.
[18] Islam S, Woyte A, Belmans R, Heskes PJM, Rooij PM. Investigating performance reliability and safety parameters of photovoltaic module inverter:

test results and compliances with the standards. Renew Energy 2006;31: 1157–81.
[19] Hamrouni N, Jraidi M, Cherif A. New control strategy for 2-stage grid-connected photovoltaic power system. Renew Energy 2008;33:2212–21.
[20] Mondol JD, Yohanis YG, Norton B. The impact of array inclination and orientation on the performance of a grid-connected photovoltaic system. Renew Energy 2007;32:118–40.
[21] Thandi GS, Zhang R, Zhing K, Lee FC, Boroyevich D. Modeling, control and stability analysis of a PEBB based DC DPS. IEEE Trans Power Deliv 1999;14:497–505.
[22] Gannet RA. Control strategies for high power four-leg voltage-source inverters. Dissertation, Virginia Tech; 2001.
[23] Ryan MJ, De Doncker RW, Lorenz RD. Decoupled control of a four-leg inverter via a new 4×4 transformation matrix. IEEE Trans Power Electr 2001;16: 694–701.
[24] Nasiri R, Radan A. Pole-placement control strategy for 4 leg voltage source inverters. In: Proceedings of the IEEE-PEDSTC '10 Conference; 2010, p. 74–79.
[25] Paraskevopoulos PN. Modern control engineering. New York: Marcel Decker; 2002.